Bioconjugate Chemistry

pubs.acs.org/bc

Article

Label-Free, Multiplex Glycan Microarray Biosensor for Influenza Virus Detection

Hanyuan Zhang, Alanna M. Klose, and Benjamin L. Miller*

Cite This: *Bioconjugate Chem.* 2021, 32, 533−540

Read Online

ACCESS | Metrics & More | Article Recommendations

ABSTRACT: Newly emerging influenza viruses adapted from animal species pose significant pandemic threats to public health. An understanding of hemagglutinin (HA) receptor-binding specificity to host receptors is key to studying the adaptation of influenza viruses in humans. This information may be particularly useful for predicting the emergence of a pandemic outbreak. Therefore, high-throughput sensing technologies able to profile HA receptor binding can facilitate studies of influenza virus evolution and adaptation in humans. As a step toward this goal, we have prepared glycan-based receptor analogue microarrays on the Arrayed Imaging Reflectometry (AIR) platform. These arrays demonstrate label-free, multiplex detection and discrimination between human and avian influenza viruses. Microarrays consisting of glycan probes with 2,6 and 2,3 linkages were prepared. After first confirming their ability to capture lectins (carbohydrate-binding proteins) with known specificities, we observed that the arrays were able to discriminate between and quantify human pandemic influenza A/California/07/2009 (H1N1pdm) and avian A/Netherlands/1/2000 (H13N8) influenza viruses, respectively. As the method may be expanded to large numbers of glycans (>100) and virus subtypes (H1−H18), we anticipate it can be applied to systematically evaluate influenza virus adaptation in humans. In turn, this will facilitate global influenza surveillance and serve as a new tool enabling health organizations, governments, research institutes, and laboratories to react quickly in the face of a pandemic outbreak.

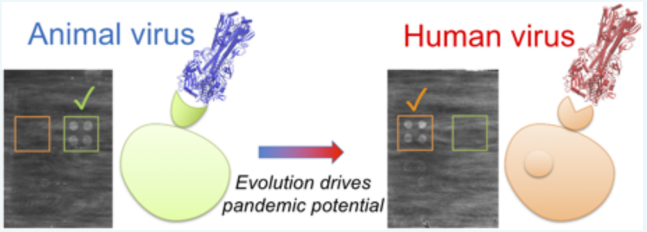

INTRODUCTION

The recent global outbreak of SARS-CoV-2 has resulted in dramatic social upheaval, clearly highlighting the potential of an animal-sourced respiratory pathogen to rapidly produce sustained human to human spread, with concomitant fatalities and significant economic damage.[1] Influenza virus, which possesses high mutation rates and adaptive abilities in different hosts and has caused both historically significant pandemics as well as seasonal infections,[2,3] requires continuing attention to its antigenic evolution and adaptation in humans. Since the early years of the last century, three hemagglutinin (HA) subtypes (H1, H2, and H3) and two neuraminidase (NA) subtypes (N1 and N2) have adapted from animal species to enable circulation among humans.[4] As a result, four significant influenza pandemics have occurred worldwide (1918 H1N1, 1957 H2N2, 1968 H3N2, and 2009 H1N1), resulting in millions of deaths and countless financial and social costs.[5−8] Since then, new animal-sourced influenza viruses including avian H5N1, H7N9, and H9N2 strains have occasionally infected humans but fortunately have not been able to spread.[9−11] However, further evolution of these viruses including gene reassortment events could lead to their full adaptation to humans with high and sustained transmission ability. In particular, the Asian lineage avian influenza H7N9 virus has achieved the largest spread, with 1,567 laboratory-confirmed human infections since it first emerged in 2013.[12,13] This has further raised the concern that an animal sourced influenza virus could trigger a pandemic outbreak.

Since HA receptor specificity is a key factor in the process of infection, transmission, and adaptation of influenza viruses, many studies have focused on understanding the influence of linkage structures of sialic acid groups in host receptor complex glycans, as these vary from species to species.[14] Human-adapted influenza HA proteins have a binding preference for α2,6 linked sialic acid moieties (*N*-acetylneuraminic acid, α2,6, galactose: abbreviated as NeuAcα2,6Gal, Figure 1), which are mostly found on the epithelial cells of the human upper respiratory tract.[15] In contrast, animal influenza HA proteins target the α2,3 linked sialic acid moieties (NeuAcα2,3Gal), which are abundant in the epithelial cells of the intestine and the whole respiratory tract of birds and other animals.[16] Many studies have demonstrated that this difference in the linkage

Received: December 31, 2020
Revised: January 19, 2021
Published: February 9, 2021

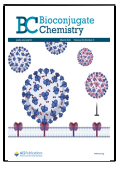

https://dx.doi.org/10.1021/acs.bioconjchem.0c00718
Bioconjugate Chem. 2021, 32, 533−540

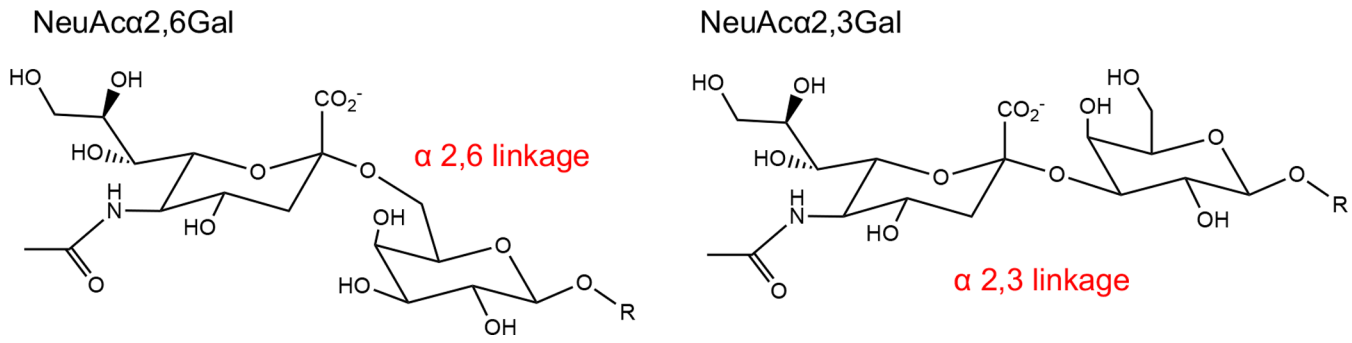

Figure 1. Structures of human and avian cell surface sialyloligosaccharides.

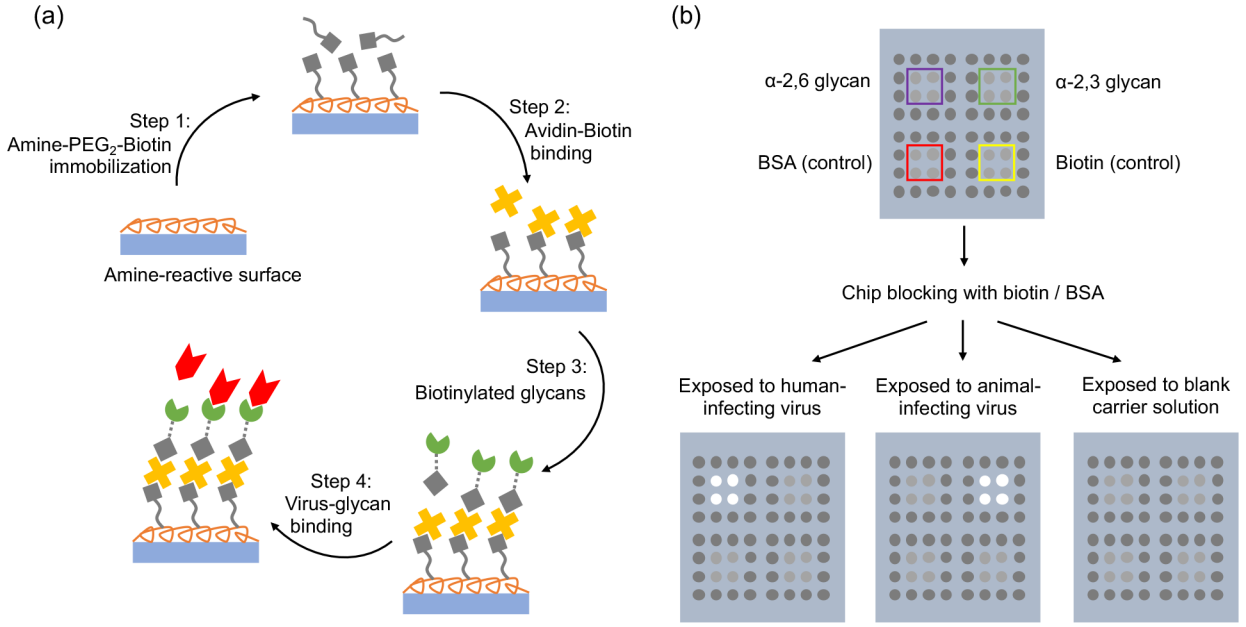

Figure 2. (a) Schematic of AIR microarray chip preparation and incubation for virus-glycan binding detection. An amine-reactive chip surface is first uniformly coated with amine-PEG_2-biotin (Step 1) and then avidin (Step 2) and stabilized. Biotinylated glycans are spotted (Step 3) completing the sensor manufacturing process. Incubation with the virus (Step 4) constitutes the assay itself. (b) Layout design of glycan-based receptor analogue microarrays and response patterns for the discrimination of human-infecting (α2,6-sialic acid binding) and avian-infecting (α2,3-sialic acid binding) influenza viruses.

structures of both sialic acids (α2,6 vs α2,3), although seemingly subtle, thus determines the ability of influenza viruses to infect different species.[17,18] While PCR is the gold-standard diagnostic technique for the presence of influenza virus, PCR cannot *a priori* determine the receptor-binding specificity of an isolated influenza virus. Therefore, sensors for rapidly identifying the HA receptor specificity, and especially discrimination of influenza HA proteins binding α2,6 and α2,3 linked sialic acids, are critical for assessing the adaptative ability of newly emerging animal influenza viruses. Such tools could facilitate the early prevention of potential influenza pandemics via rapid characterization of viral isolates.[19]

The availability of synthetic glycans in different formats has led to their extensive application in microarray platforms.[20−22] These synthesized glycans or "receptor-binding analogues" can be immobilized on substrates for characterization of influenza virus specificity at varying levels of throughput.[23] In particular, microarrays developed by the Consortium for Functional Glycomics (CFG)[24] include several hundred covalently immobilized glycans ranging in size and functionality, thus offering the opportunity to systematically investigate the influenza HA specificity to a large number of glycans. However, methods used to evaluate influenza HA glycan binding have primarily employed an ELISA-type format, with multistep workflows and fluorescent reporter reagents. Although some label-free biosensing technologies have been applied to measure binding avidity of HAs to glycan analogues, as far as we are aware none have been implemented in a multiplex format.[25−27] Therefore, label-free sensor technologies able to rapidly profile influenza HA glycan binding specificity in a microarray format are highly desirable.

To address this need, we have prepared and tested microarrays of influenza receptor-binding analogues on the Arrayed Imaging Reflectometry (AIR) sensor platform. AIR is a label-free, multiplex detection solution. The platform utilizes a single-camera interferometric imaging setup, in which s-polarized light from a HeNe laser (632.8 nm) is expanded and collimated to illuminate arrays prepared on silicon/silicon dioxide substrates. The reflected image of the array is captured by a charge-coupled device (CCD) camera. The thickness of the chips and microarrayed biomolecules is controlled precisely in order to create a near-perfect antireflection

https://dx.doi.org/10.1021/acs.bioconjchem.0c00718
Bioconjugate Chem. 2021, 32, 533−540

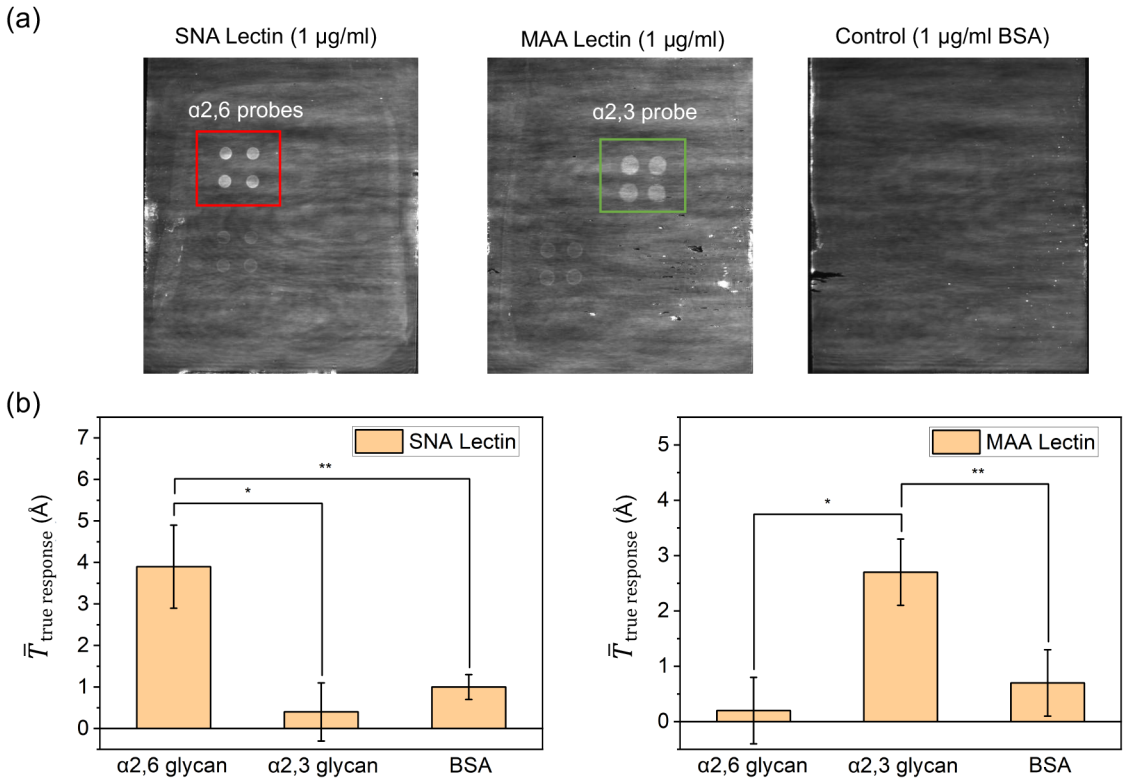

Figure 3. (a) AIR microarray images (250 ms exposure) of α2,6 linked, α2,3 linked, b-BSA, and biotin probe spots for the discrimination of SNA and MAA lectin proteins. (b) Quantitative results of the microarray response against SNA and MAA lectin proteins.

condition in the absence of target molecule binding.[28] Binding of the analyte of interest to a capture spot results in a thickness change that perturbs the antireflection condition, resulting in light reflecting in proportion to the amount of material captured. The utility of AIR has been demonstrated in a broad range of applications, including detection and quantification of cytokines and other inflammatory biomarkers in human serum,[29] antibodies to human autoantigens,[30] and as a real-time method for monitoring protein-RNA binding.[31] Recently, we have also used the technique as a method for analyzing the human response to SARS-CoV-2 (COVID-19) infection.[32]

In the context of influenza, we have used arrays of hemagglutinins (HAs) to monitor the human[33] and avian[34] immune response to influenza infection or vaccination with AIR. AIR microarray biosensors consisting of a library of vaccine derived human monoclonal antibodies (up to 115-plex) have proven useful for serotyping influenza virus subtypes and showed the potential of systematically mapping the antigenic binding epitopes based on the array's response patterns.[35−37] To extend the methodology to HA receptor binding, we report here a glycan-based AIR biosensor with α2,6 and α2,3 linked sialic acid polymeric receptor-binding analogues. This array is able to bind and discriminate between human- and avian-infectious influenza viruses. In addition to demonstrating the first use of carbohydrate capture molecules on the AIR platform, this work provides proof-of-concept for multiplex AIR arrays to help increase our understanding of influenza biology, particularly to promote the prediction of viral adaptation across species.

RESULTS

The workflow of microarray chip preparation and polymer-based glycan-antigen detection is illustrated in Figure 2(a). A stable biotin−avidin layer was first prepared on the amine-reactive silicon/SiO_2 chips to enable immobilization of the biotinylated glycan probes.[38] The commercial glycan receptor analogues are synthesized on a polyacrylamide (PAA) polymer carrier; this acts as a spacer between the sensing surface of the chip and sialic acid moieties, limiting steric interactions with the surface and enabling unbiased interactions.[39] Because AIR is an interferometric method rather than a technique reliant on an evanescent field (as surface plasmon resonance is, for example), use of a linker does not decrease detection sensitivity. Figure 2(b) shows the microarray layout. To complement α2,6 linked glycan (purple boxed) and α2,3 linked glycan (green boxed) probe spots, biotinylated bovine serum albumin (b-BSA) (red boxed) and D-biotin (yellow boxed) spots were used at the lower sections as on-chip controls for nonspecific binding. In addition, 12 replicate spots of biotinylated polyacrylamide carbohydrate probes lacking sialic acid (galactose-beta-1,4-*N*-acetylglucosamine-beta-poly-acrylamide-biotin, Galb1−4GlcNAcb-PAA-biotin) were printed surrounding each subsection of the microarray to correct for any local changes in chip thickness. Prior to assay, the chips were blocked first with 0.1 mg/mL D-biotin solutions in PBS buffer and then BSA in sodium acetate. The prepared and blocked chips were then exposed to the target protein or virus for the next steps. Control experiments used blank carrier solutions lacking the target antigen.

To confirm that glycans immobilized on the array retain their expected specificity, we first tested binding of glycan-binding proteins (lectins). *Sambucus nigra* (SNA) and *Maackia*

https://dx.doi.org/10.1021/acs.bioconjchem.0c00718
Bioconjugate Chem. 2021, 32, 533−540

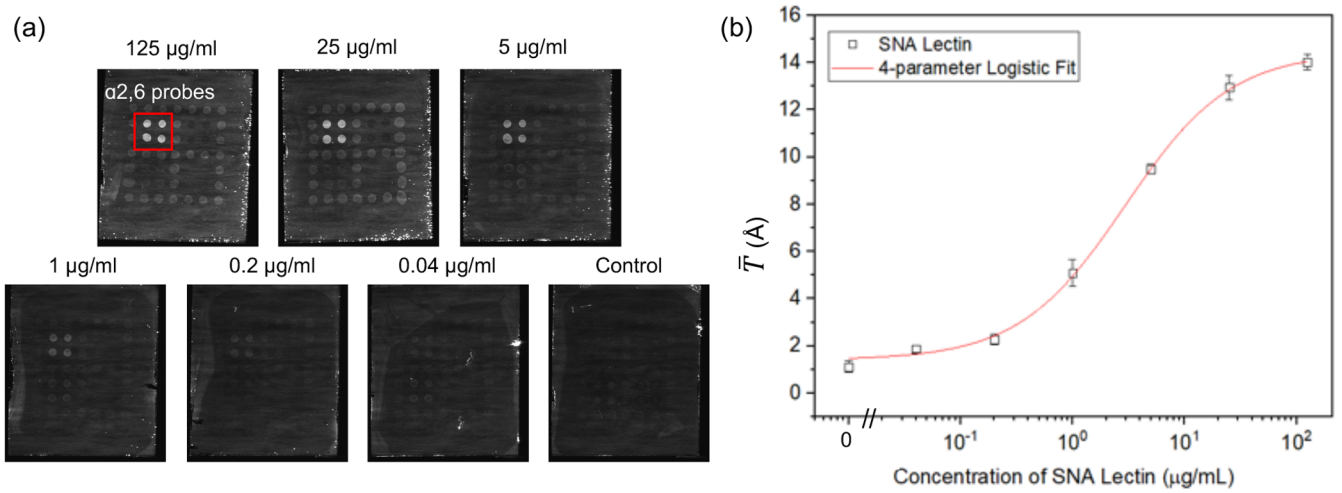

Figure 4. (a) AIR microarray images (100 ms exposure) following exposure to serial dilutions of SNA lectin protein. (b) Concentration-dependent response data for SNA lectin binding to the array. The red line is a 4-parameter logistic fit of the response at each concentration (adjusted R^2: 0.99).

amurensis (MAA) lectin proteins are known to be specific for binding α2,6 and α2,3 linked glycans, respectively.[40,41] Figure 3(a) shows experimental results for the discrimination of SNA and MAA lectin proteins spiked in the PBS solution at a concentration of 1 μg/mL. The highlighted bright spots (red boxed) in the AIR image for SNA lectin detection demonstrate a positive response of the α2,6 linked glycan probe spots. The α2,3 linked glycan probe spots are muted indicating that the SNA lectin proteins were selectively captured by α2,6 linked glycan probe spots. In contrast, the highlighted spots (green boxed) in the AIR image for target MAA lectin protein demonstrate a strong positive response of only α2,3 linked glycan probes, while the α2,6 linked glycan probes are muted. In addition, the overall probe morphologies of the AIR images are uniform, with no "coffee ring" artifacts. This indicates that the surface chemistry and immobilization protocols behave as desired.

AIR microarray images also provide quantitative information regarding the binding affinity and the amount of captured target. In Figure 3(b), the quantitative response data represented by the increase of the thickness (in Å) of the captured materials on the microarray confirm the qualitative observations from Figure 3(a). Differences between the positive responses of the α2,6 linked glycan probe spots and the negative responses of α2,3 linked glycan probe spots were statistically significant, with p-values of 0.009 (<0.05) for SNA detection and 0.007 (<0.05) for MAA detection. Nonspecific binding to the b-BSA probe spots was also significantly lower than to positive probe spots (both p-values are 0.002 < 0.05). These results confirm the high selectivity of the glycan microarrays for their specific lectin proteins.

To confirm that lectin binding to the array was analytically well behaved, we tested the response of microarrays exposed to a serial dilution of SNA lectin protein in PBS. The response data of the α2,6 linked glycan probe spots (red boxed) in Figure 4(a) following exposure to concentrations of SNA ranging from 0.04 to 125 μg/mL are plotted in Figure 4(b). A concentration-dependent 4-parameter logistic equation was used to fit the data, yielding an adjusted R^2 value of 0.99. The limit of detection, defined based on three times the standard deviation of the lowest measurement, was found to be 0.06 μg/mL with a 95% confidence interval. This provides an overall detection range of 4 logs in concentration. The overall response curve and observed SNA binding affinity are similar to previously published single-channel SPR data for SNA lectin binding an immobilized α2,6 sialoside.[40]

To assess the ability of the glycan-based microarray biosensor to detect and discriminate live human and avian influenza viruses, we incubated the microarrays with selected pseudotyped influenza viruses spiked at 10^6 pfu/mL in 10% FBS solutions overnight and measured the probe responses relative to the control chips. Pseudotyped, or single-cycle, infectious influenza A viruses are recombinant strains in which the hemagglutinin (HA) gene is deleted or replaced with a fluorescent marker such as GFP or mCherry.[42] As such, they can only replicate when cotransfected with an HA expressing plasmid and are therefore safe to handle in the laboratory at a low biosafety level. Results for these experiments are shown in Figure 5. Human influenza H1N1pdm bound to the α2,6 linked glycan probe spots with high selectivity, as expected for this virus. Likewise, the avian influenza H13N8 virus only bound to the α2,3 linked glycan probe spots, consistent with its species specificity. In both cases, the microarray response image obtained from exposure to 1 μg/mL of BSA spiked in 10% FBS solution was used as the control. Quantified response data (Figure 5(b)) confirms specific binding of the virus to each glycan probe for human (red boxed) and avian (green boxed) influenza viruses, respectively. Significant differences between the binding responses of the analyte probe spots and the control groups were obtained, with p-values of 0.029 (<0.05) for the human H1N1pdm influenza virus and 0.012 (<0.05) for the avian H13N8 influenza virus.

The dynamic range of the glycan microarray was also tested via exposure to serial dilutions of the human influenza H1N1pdm virus stock (10^8 pfu/mL) spiked with 10% FBS. The AIR microarray images were captured (Figure 5(c)), recorded, and analyzed for quantitative responses as shown in Figure 5(d). Each probe spot (red boxed) was further resolved for estimating the bound human H1N1pdm virus. Analysis of the resulting response curve indicates a lower limit of detection of 9.29×10^5 pfu/mL or a 3 orders of magnitude dynamic range for detection. This is an order of magnitude lower than that observed for SNA lectin and is a direct result of the increased standard deviations observed for each virus

https://dx.doi.org/10.1021/acs.bioconjchem.0c00718
Bioconjugate Chem. 2021, 32, 533−540

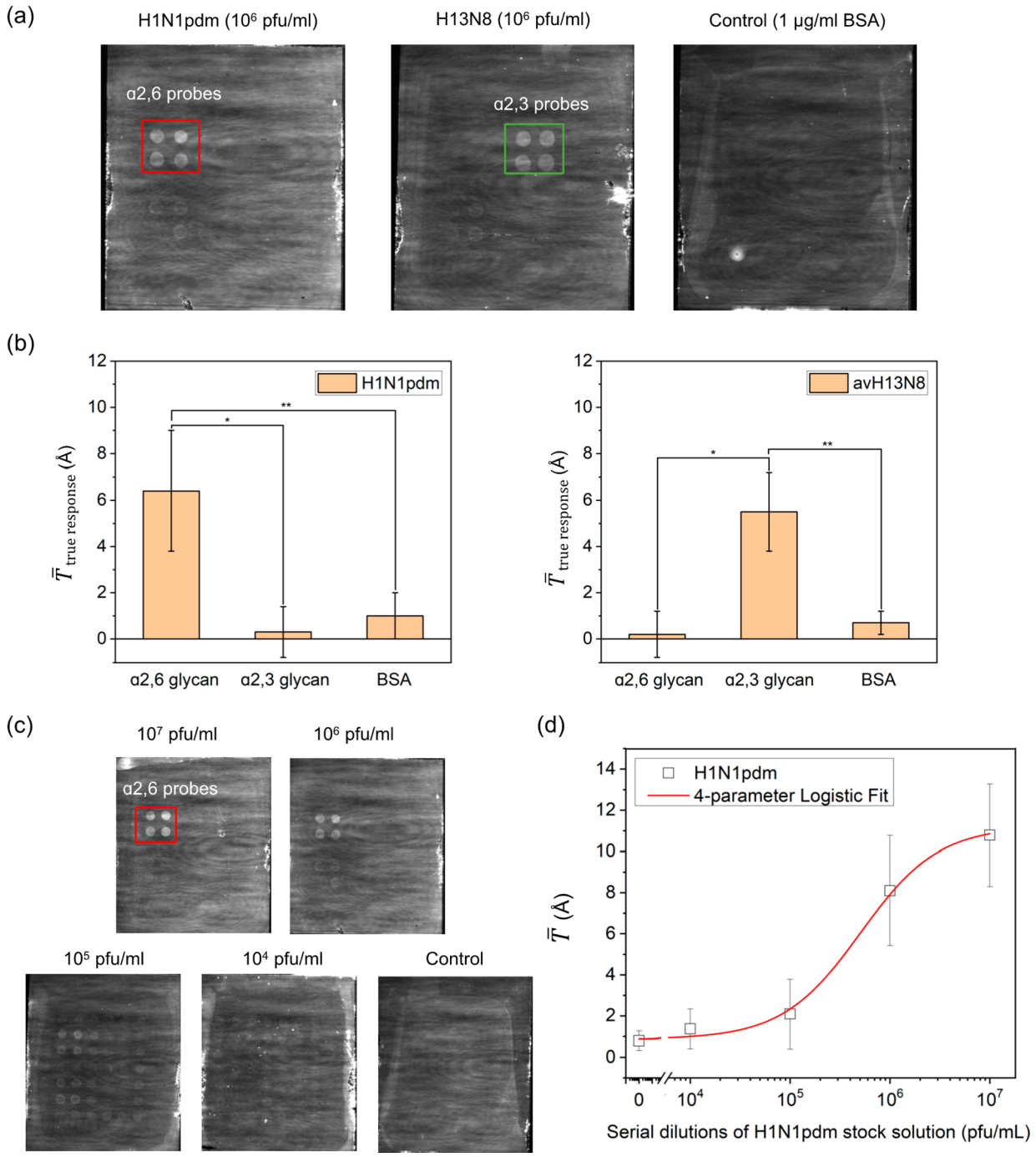

Figure 5. Responses of the AIR glycan microarray to human influenza H1N1pdm and avian influenza H13N8 viruses. (a) Images for arrays exposed to H1N1pdm (left), H13N8 (center), and a control sample (right). (b) Quantitative response data of the glycan microarray to the human influenza H1N1pdm virus (left) and avian influenza H13N8 virus (right). (c) AIR images (250 ms exposure) show chip response in (d) at varying concentrations of the virus.

concentration. Further optimization of the assay protocol may allow for improvement in both the detection limit and dynamic range. However, we note that the observed performance is more than sufficient to enable discrimination of binding to different receptor glycan analogues (as in Figure 5a), the primary goal for the assay.

DISCUSSION

The prevention of influenza pandemics is a significant endeavor that requires close and efficient collaboration across broad scientific fields including bioengineering, immunology, virology, bioinformatics, and medicine. Influenza pandemics usually originate from an animal-sourced virus that has acquired the ability of consistent transmission among humans. In the fight against such an outbreak, time is a very limited commodity. Currently, the front line of a pandemic is defended by health organizations and governments which provide strategies for developing vaccines and treatment guidelines. However, the lengthy process of producing effective vaccines can delay resolution of the pandemic, resulting in significant

https://dx.doi.org/10.1021/acs.bioconjchem.0c00718
Bioconjugate Chem. 2021, 32, 533−540

casualties. Our previous work used an antibody microarray biosensor to demonstrate an effective strategy for responding quickly to an emerging pandemic outbreak by identifying known antigenically similar vaccine strains of influenza to facilitate the vaccine discovery process.[36] This approach was further tested and found to be useful in a national (USA) mock pandemic exercise.[37] The work described here is intended to enable the identification of human-infecting (and potentially pandemic) virus strains as they evolve from an animal source before they become pandemic, thereby allowing a public health response at an even earlier time point.

To that end, we have successfully demonstrated glycan-based microarray biosensors on the AIR platform that easily and effectively discriminates between animal- and human-infective influenza viruses based on their HA receptor glycan specificity. Microarrays with immobilized 2,6 and 2,3 linked glycan analogues were capable of label-free and multiplex detection of glycan-binding lectin proteins and discrimination between the human influenza A/California/07/2009 H1N1pdm strain and avian sourced influenza A/Netherlands/1/2000 H13N8 virus. We observed an unoptimized lower limit of detection of 0.06 μg/mL for the lectins, and arrays were analytically well behaved, exhibiting a concentration dependent response consistent with Langmuir binding behavior. The unoptimized detection limit for the H1N1pdm virus was 9.29×10^5 pfu/mL. While optical sensors have been described with single-particle detection sensitivity for influenza,[43] our observed sensitivity is more than sufficient for the envisioned application. AIR provides several advantages over traditional immunoassay formats such as ELISA including a much simpler workflow. As a multiplex technique, AIR provides much higher data throughput than either singleplex ELISA or single-channel surface plasmon resonance (SPR) assays, with comparable or better sensitivity. Finally, since the performance of AIR is independent of plex (i.e., the number of different analytes captured on the array), we expect that it will be straightforward to expand this microarray to large numbers of glycans for systematically investigating the receptor specificity of influenza subtypes from many different species. Such an array will significantly facilitate global virus surveillance and efforts to prevent future outbreaks of pandemic influenza.

MATERIALS AND METHODS

Materials and Reagents. Amine-reactive AIR substrates (5 × 6 mm) were purchased from Adarza BioSystems, Inc. D-Biotin and EZ-Link amine-PEG_2-biotin were purchased from ThermoFisher Scientific. Avidin was purchased from Rockland Immunochemicals, Inc. Pseudotyped influenza viruses (A/California/07/2009 H1N1pdm and avian A/Netherlands/1/2000 H13N8) were a gift of Prof. Luis Martinez-Sobrido and were prepared as previously described.[44] Biotinylated polyacrylamide (PAA) carbohydrate molecules (3′-sialyllactose-PAA-biotin 01-038, 6′-sialyllactose-PAA-biotin 01-039, and Galb1−4GlcNAcb-PAA-biotin 01-022) were purchased from GlycoTech. Biotinylated bovine serum albumin (b-BSA) was purchased from Rockland Immunochemicals, Inc. Fetal bovine serum (FBS) was purchased from Gibco by ThermoFisher Scientific.

Chip Preparation and Functionalization. First, amine-reactive silicon/SiO_2 chips were incubated with amine-PEG_2-biotin (1 mg/mL) in 1× PBS solution (PBS: 137 mM NaCl, 2.7 mM KCl, 10 mM Na_2HPO_4, and 1.76 mM KH_2PO_4−H_2O, pH 7.4) overnight, with agitation on a rotating platform shaker, at room temperature. Next, chips were washed in Assay Wash Buffer (AWB: mPBS (150 mM NaCl, 10 mM Na_2HPO_4, 10 mM NaH_2PO_4) with 0.005% tween-20, pH 7.2) for 5 min before incubation in 40 μg/mL avidin in PBS for 1 h and shaking, at room temperature. After batch-rinsing the chips for 5 min in AWB, they were incubated in a 1% solution of StabilCoat Plus in 18 MΩ-cm water produced by a Barnstead Nanopure II purification system (Nanopure) for 20 min before being spun dry for 1 min at 500 rpm after being attached to the rotating platform of a wafer polisher (Ecomet 4, Buehler, IL, USA).

Biotinylated polymer-based carbohydrate probes were suspended at a concentration of 250 μg/mL in 10 mM phosphate-buffered saline (PBS) at pH 7.0. Prepared probe solutions were spotted at a droplet volume of 250 pL using a piezoelectric arrayer (Scienion S3). Four replicate spots were printed for each type of carbohydrate probe. Twelve replicate spots of carbohydrate probes lacking the sialic acid moiety were printed adjacent to and surrounding each group of probe spots as negative controls for nonspecific binding and intrachip thickness variation. Biotinylated BSA (250 μg/mL) and D-biotin (1 mg/mL) solutions prepared in PBS were also printed on the array as negative controls. All spots were printed with a center-to-center distance of 300 μm.

Assay Protocols. Experiments with glycan-binding lectin proteins (used to confirm the specificity of immobilized probes) and pseudotyped influenza viruses followed the same general procedure. Two blocking solutions consisting of (1) 0.1 mg/mL D-biotin in 10 mM PBS and (2) 10 mg/mL BSA in sodium acetate buffer (50 mM at pH 5.0) were prepared and added to separate rows of a 96-well plate. After being incubated in BSA blocking solutions, the chips were washed in modified PBS-EDTA-Tween 20 (10 mM PBS, 5 mM EDTA, and 0.5% Tween 20 at pH 7.4) assay wash buffer (AWB) thoroughly and then transferred into a BSA preblocked row for target exposure. Solutions of lectin proteins were prepared at a concentration of 1 μg/mL in PBS. Viral titers of human and avian pseudotyped influenza viruses were reconstituted to 10^6 plaque forming units (pfu)/mL in 10% FBS solutions for target exposure or serially diluted in 10% FBS from a 10^8 pfu/mL stock. Blank 10% FBS solutions were used as negative control groups. Three chips were used per condition and incubated overnight at room temperature. After incubation, all chips were washed in AWB several times and rinsed in deionized, glass-distilled water. Finally, chips were dried under a stream of nitrogen gas prior to imaging.

Data Acquisition and Analysis. Dried chips were imaged immediately on a prototype AIR reader (Adarza BioSystems, Inc.). AIR images were acquired in a 16-bit TIFF format with an exposure time of 100 or 250 ms for lectin detection and 250 ms for virus detection. Optimal exposure time is dictated by the concentration of the analyte. At low concentration, sensitivity may be enhanced by increasing the exposure time, while at high concentration, shorter exposures are often required to prevent saturation of the detector. Multiple exposures may be obtained for each sample if desired. The AIR images were then analyzed using NIH-ImageJ (version 1.46r). Where necessary, contrast enhancement was used to locate spots; all quantitative data was obtained from unaltered images. Final plots and 4-parameter logistic regression fits were generated in OriginPro 2020 (OriginLab Corporation). The response of the biotinylated glycan probes lacking sialic acid

https://dx.doi.org/10.1021/acs.bioconjchem.0c00718
Bioconjugate Chem. 2021, 32, 533−540

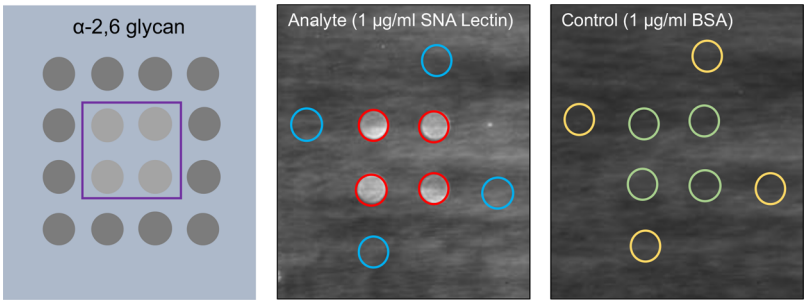

$$\bar{T}_{analyte} = \frac{\sum_{i=1}^{n}(x_i - \bar{c})}{n} \qquad \bar{T}_{control} = \frac{\sum_{i=1}^{n}(x_i - \bar{c})}{n}$$

$$\bar{T}_{true\ response} = \bar{T}_{analyte} - \bar{T}_{control}$$

Figure 6. Analysis protocol for AIR images. $\bar{T}_{analyte}$ is the average corrected analyte probe thickness, $\bar{T}_{control}$ is the average corrected control probe thickness, x is the median intensity converted thickness of a single test probe, $\bar{c}$ is the average median intensity converted thickness of four replicate correction probes surrounding each test probe, and n is the number of test probes. A contrast-enhanced image was used to locate the spots in the control.

moieties was used as a control for nonspecific binding to determine the true response data of the other probe spots. For each array spot, the response values were calculated by converting the reflection intensity unit to thickness based on an experimentally derived reference response model.[28,36] The reference response model plots the relationship between reflected intensities acquired for different exposures (100 to 500 ms) and their corresponding thicknesses as measured by ellipsometry. For each spot, a median value was obtained from the histogram of the pixel intensities measured by ImageJ, and then four median values of the four replicate spots of the same probe were averaged and used as the true response data after correcting for the response of the control chip. This procedure is illustrated in Figure 6, using a chip carrying the α2,6 glycan analogue and incubated with SNA lectin as an example. A two-sample t test was applied to analyze the response data, and a P-value cutoff of 0.05 was used to evaluate the significance of the differences between positive and negative groups. The standard deviations of replicate spots for each analyte concentration of both control and analyte chips were used to determine the error bars. All experiments were repeated twice to confirm observations.

AUTHOR INFORMATION

Corresponding Author

Benjamin L. Miller − *Materials Science Program, University of Rochester, Rochester, New York 14627, United States; Department of Dermatology, University of Rochester Medical Center, Rochester, New York 14642, United States;* orcid.org/0000-0001-9168-8047; Email: Benjamin_miller@urmc.rochester.edu

Authors

Hanyuan Zhang − *Materials Science Program, University of Rochester, Rochester, New York 14627, United States; Department of Dermatology, University of Rochester Medical Center, Rochester, New York 14642, United States*

Alanna M. Klose − *Department of Dermatology, University of Rochester Medical Center, Rochester, New York 14642, United States*

Complete contact information is available at: https://pubs.acs.org/10.1021/acs.bioconjchem.0c00718

Notes

The authors declare no competing financial interest.

ACKNOWLEDGMENTS

We thank Prof. Luis Martínez-Sobrido for generously donating pseudotyped influenza viruses. This project has been funded in whole or in part with Federal funds from the National Institute of Allergy and Infectious Diseases, National Institutes of Health, Department of Health and Human Services, under CEIRS Contract No. HHSN272201400005C.

REFERENCES

(1) COVIDView Weekly Summary Updated August 14, 2020, Centers for Disease Control and Prevention (CDC). https://www.cdc.gov/coronavirus/2019-ncov/covid-data/covidview/index.html (accessed 2020-08-16).

(2) Webster, R. G., Bean, W. J., Gorman, O. T., Chambers, T. M., and Kawaoka, Y. (1992) Evolution and ecology of influenza A viruses. *Microbiol. Rev. 56*, 152−179.

(3) Taubenberger, J. K., and Kash, J. C. (2010) Influenza virus evolution, host adaptation, and pandemic formation. *Cell Host Microbe 7*, 440−451.

(4) Neumann, G., and Kawaoka, Y. (2006) Host range restriction and pathogenicity in the context of influenza pandemic. *Emerging Infect. Dis. 12*, 881.

(5) Reid, A. H., Fanning, T. G., Hultin, J. V., and Taubenberger, J. K. (1999) Origin and evolution of the 1918 "Spanish" influenza virus hemagglutinin gene. *Proc. Natl. Acad. Sci. U. S. A. 96*, 1651−1656.

(6) Joseph, U., Linster, M., Suzuki, Y., Krauss, S., Halpin, R. A., Vijaykrishna, D., Fabrizio, T. P., Bestebroer, T. M., Maurer-Stroh, S., Webby, R. J., et al. (2015) Adaptation of pandemic H2N2 influenza A viruses in humans. *J. Virol. 89*, 2442.

(7) Kilbourne, E. D. (2006) Influenza pandemics of the 20th century. *Emerging Infect. Dis. 12*, 9.

(8) Al-Muharrmi, Z. (2010) Understanding the influenza A H1N1 2009 pandemic. *Sultan Qaboos University Medical Journal 10*, 187−195.

(9) Claas, E. C., Osterhaus, A. D., Van Beek, R., De Jong, J. C., Rimmelzwaan, G. F., Senne, D. A., Krauss, S., Shortridge, K. F., and Webster, R. G. (1998) Human influenza A H5N1 virus related to a highly pathogenic avian influenza virus. *Lancet 351*, 472−477.

(10) Gao, R., Cao, B., Hu, Y., Feng, Z., Wang, D., Hu, W., Chen, J., Jie, Z., Qiu, H., Xu, K., et al. (2013) Human infection with a novel

avian- origin influenza A (H7N9) virus. *N. Engl. J. Med. 368*, 1888−1897.
(11) Peiris, M., Yuen, K., Leung, C., Chan, K., Ip, P., Lai, R., Orr, W., and Shortridge, K. (1999) Human infection with influenza H9N2. *Lancet 354*, 916−917.
(12) Kile, J. C., Ren, R., Liu, L., Greene, C. M., Roguski, K., Iuliano, A. D., Jang, Y., Jones, J., Thor, S., and Song, Y. (2017) Update: increase in human infections with novel Asian lineage avian influenza A (H7N9) viruses during the fifth epidemic-China, October 1, 2016-August 7, 2017. *MMWR. Morbidity and mortality weekly report 66*, 928−932.
(13) Human infection with avian influenza A(H7N9) virus − China: Update, September 5, 2018. https://www.who.int/csr/don/05-september-2018-ah7n9-china/en/ (accessed 2020-08-14).
(14) Weis, W., Brown, J. H., Cusack, S., Paulson, J. C., Skehel, J. J., and Wiley, D. C. (1988) Structure of the influenza virus haemagglutinin complexed with its receptor, sialic acid. *Nature 333*, 426−431.
(15) Matrosovich, M. N., Matrosovich, T. Y., Gray, T., Roberts, N. A., and Klenk, H.-D. (2004) Human and avian influenza viruses target different cell types in cultures of human airway epithelium. *Proc. Natl. Acad. Sci. U. S. A. 101*, 4620−4624.
(16) Shinya, K., Ebina, M., Yamada, S., Ono, M., Kasai, N., and Kawaoka, Y. (2006) Avian flu: influenza virus receptors in the human airway. *Nature 440*, 435.
(17) Viswanathan, K., Chandrasekaran, A., Srinivasan, A., Raman, R., Sasisekharan, V., and Sasisekharan, R. (2010) Glycans as receptors for influenza pathogensis. *Glycoconjugate J. 27*, 561−570.
(18) Byrd-Leotis, L., Jia, N., Dutta, S., Trost, J. F., Gao, C., Cummings, S. F., Braulke, T., Müller-Loennies, S., Heimburg-Molinaro, J., Steinhauer, D. A., et al. (2019) Influenza binds phosphorylated glycans from human lung. *Sci. Adv. 5*, eaav2554.
(19) Taubenberger, J. K., and Morens, D. M. (2008) The pathology of influenza virus infections. *Annu. Rev. Pathol.: Mech. Dis. 3*, 499−522.
(20) Stevens, J., Blixt, O., Paulson, J. C., and Wilson, I. A. (2006) Glycan microarray technologies: tools to survey host specificity of influenza viruses. *Nat. Rev. Microbiol. 4*, 857.
(21) Stevens, J., Blixt, O., Glaser, L., Taubenberger, J. K., Palese, P., Paulson, J. C., and Wilson, I. A. (2006) Glycan microarray analysis of the hemagglutinins from modern and pandemic influenza viruses reveals different receptor specificities. *J. Mol. Biol. 355*, 1143−1155.
(22) de Paz, J. L., and Seeberger, P. H. (2012) In *Carbohydrate Microarrays*, Springer, pp 1−12, DOI: 10.1007/978-1-61779-373-8_1.
(23) McQuillan, A. M., Byrd-Leotis, L., Heimburg-Molinaro, J., and Cummings, R. D. (2019) Natural and synthetic sialylated glycan microarrays and their applications. *Front. Mol. Biosci. 6*, 88.
(24) Blixt, O., Head, S., Mondala, T., Scanlan, C., Huflejt, M. E., Alvarez, R., Bryan, M. C., Fazio, F., Calarese, D., and Stevens, J. (2004) Printed covalent glycan array for ligand profiling of diverse glycan binding proteins. *Proc. Natl. Acad. Sci. U. S. A. 101*, 17033−17038.
(25) Xiong, X., Martin, S. R., Haire, L. F., Wharton, S. A., Daniels, R. S., Bennett, M. S., McCauley, J. W., Collins, P. J., Walker, P. A., Skehel, J. J., et al. (2013) Receptor binding by an H7N9 influenza virus from humans. *Nature 499*, 496.
(26) Suenaga, E., Mizuno, H., and Penmetcha, K. K. R. (2012) Monitoring influenza hemagglutinin and glycan interactions using surface plasmon resonance. *Biosens. Bioelectron. 32*, 195−201.
(27) Fei, Y., Sun, Y. S., Fei, Y., Sun, Y. S., Li, Y., Yu, H., Lau, K., Landry, J. P., Luo, Z., Baumgarth, N., et al. (2015) Characterization of Receptor Binding Profiles of Influenza A Viruses Using An Ellipsometry-Based Label-Free Glycan Microarray Assay Platform. *Biomolecules 5*, 1480−1498.
(28) Mace, C. R., Striemer, C. C., and Miller, B. L. (2006) Theoretical and experimental analysis of arrayed imaging reflectometry as a sensitive proteomics technique. *Anal. Chem. 78*, 5578−5583.
(29) Mace, C. R., Striemer, C. C., and Miller, B. L. (2008) Detection of human proteins using arrayed imaging reflectometry. *Biosens. Bioelectron. 24*, 334−337.
(30) Bucukovski, J., Carter, J. A., Striemer, C. C., Müllner, S., Schulte-Pelkum, J., Schulz-Knappe, P., and Miller, B. L. (2018) Label-free microarray-based detection of autoantibodies in human serum. *J. Immunol. Methods 459*, 44−49.
(31) Yadav, A. R., Mace, C. R., and Miller, B. L. (2014) Examining the interactions of the splicing factor MBNL1 with target RNA sequences via a label-free, multiplex method. *Anal. Chem. 86*, 1067−1075.
(32) Steiner, D. J., Cognetii, J. S., Luta, E. P., Klose, A. M., Bucukovski, J., Bryan, M. R., Schmuke, J. J., Nguyen-Contant, P., Sangster, M. Y., Topham, D. J., et al. (2020) Array-based analysis of SARS-CoV-2, other coronaviruses, and influenza antibodies in convalescent COVID-19 patients. *Biosens. Bioelectron. 169*, 112643.
(33) Mace, C. R., Topham, D. J., Mosmann, T. R., Quataert, S. A., Treanor, J. J., and Miller, B. L. (2011) Label-free, arrayed sensing of immune response to influenza antigens. *Talanta 83*, 1000−1005.
(34) Bucukovski, J., Latorre-Margalef, N., Stallknecht, D. E., and Miller, B. L. (2015) A multiplex label-free approach to avian influenza surveillance and serology. *PLoS One 10*, e0134484.
(35) Zhang, H., Dunand, C. H., Wilson, P., and Miller, B. L. (2016) A label-free optical biosensor for serotyping "unknown" influenza viruses. *Proc. SPIE*, 982405.
(36) Zhang, H., Henry, C., Anderson, C. S., Nogles, A., DeDiego, M. L., Bucukovski, J., Martinez-Sobrido, L., Wilson, P. C., Topham, D. J., and Miller, B. L. (2018) Crowd on a chip: Label-free human monoclonal antibody arrays for serotyping influenza. *Anal. Chem. 90*, 9583−9590.
(37) Martinez-Sobrido, L., Blanco-Lobo, P., Rodriguez, L., Fitzgerald, T., Zhang, H., Nguyen, P., Anderson, C. S., Holden-Wiltse, J., Bandyopadhyay, S., Nogales, A., et al. (2020) Characterizing emerging canine H3 influenza viruses. *PLoS Pathog. 16*, e1008409.
(38) Klose, A., and Miller, B. L. (2020) A stable biotin-streptavidin surface enables multiplex, label-free protein detection by aptamer and aptamer-protein arrays using Arrayed Imaging Reflectometry. *Sensors 20*, 5745.
(39) Reimhult, E., and Höök, F. (2015) Design of Surface Modifications for Nanoscale Sensor Applications. *Sensors 15*, 1635−1675.
(40) Linman, M. J., Taylor, J. D., Yu, H., Chen, X., and Cheng, Q. (2008) Surface plasmon resonance study of protein-carbohydrate interactions using biotinylated sialosides. *Anal. Chem. 80*, 4007−4013.
(41) Nicholls, J. M., Bourne, A. J., Chen, H., Guan, Y., and Peiris, J. M. (2007) Sialic acid receptor detection in the human respiratory tract: evidence for widespread distribution of potential binding sites for human and avian influenza viruses. *Respir. Res. 8*, 73.
(42) Nogales, A., Baker, S. F., Domm, W., and Martínez-Sobrido, L. (2016) Development and applications of single-cycle infectious influenza A virus (scIAV). *Virus Res. 216*, 26−40.
(43) Vollmer, F., Arnold, S., and Keng, D. (2008) Single virus detection from the reactive shift of a whispering-gallery mode. *Proc. Natl. Acad. Sci. U. S. A. 105*, 20701−20704.
(44) Nogales, A., Baker, S. F., and Martinez-Sobrido, L. (2015) Replication-competent influenza A viruses expressing a red fluorescent protein. *Virology 476*, 206−216.

https://dx.doi.org/10.1021/acs.bioconjchem.0c00718
Bioconjugate Chem. 2021, 32, 533−540